Hindawi
Mathematical Problems in Engineering
Volume 2019, Article ID 5173956, 10 pages
https://doi.org/10.1155/2019/5173956

Research Article

Robust Prediction Algorithm Based on a General EIV Model for Multiframe Transformation

Lihui Yao [1,2], Peng Lin [3], Jingxiang Gao [1,2], and Chao Liu [4]

[1] *NASG Key Laboratory of Land Environment and Disaster Monitoring, China University of Mining and Technology, Xuzhou 221116, Jiangsu, China*
[2] *School of Environment Science and Spatial Informatics, China University of Mining & Technology, Xuzhou 221116, Jiangsu, China*
[3] *College of Civil Engineering, Anhui Jianzhu University, Hefei 230000, Anhui, China*
[4] *School of Geodesy and Geomatics, Anhui University of Science and Technology, Huainan 232001, Anhui, China*

Correspondence should be addressed to Jingxiang Gao; jxgao@cumt.edu.cn

Received 15 November 2018; Revised 6 January 2019; Accepted 30 January 2019; Published 11 February 2019

Academic Editor: Jixiang Yang

In modern geodesy, there are cases in which the target frame is unique and there is more than one source frame. Helmert transformations, which are extensively used to solve transformation parameters, can be separately solved between the target frame and one of the source frames. However, this is not globally optimal, even though each transformation is locally optimal on its own. Additionally, this also generates the problem of multiple solutions in the noncommon station of the target frame. Moreover, least squares solutions can cause estimation value distortion, with a gross error existing in observations. Thus, in this paper, Helmert transformations among three frames, that is, one target frame and two source frames, are studied as an example. A robust prediction algorithm based on the general errors-in-variables prediction algorithm and the robust estimation is derived in detail and is applied to achieve multiframe total transformation. Furthermore, simulation experiments were conducted and the results validated the superiority of the proposed total transformation method over classical separate approaches.

1. Introduction

The precision and reliability of terrestrial reference frames have improved with the rapid development of the Global Navigation Satellite System (GNSS) [1]. At present, common terrestrial reference frames include WGS-84, PE-90, CGCS-2000, and ITRF2008. The three-dimensional (3D) space coordinates of ground control points in the source coordinate system are obtained using GNSS observations, whereas local coordinate systems are often used for geodetic surveying. Therefore, it is necessary to use coordinate transformation to unify the data. Similarity datum transformation is widely used in 3D coordinate transformation. Common point coordinates are typically used to solve the transformation parameters, and then the coordinates of noncommon points in the old coordinate system are converted to the new coordinate system according to the transformation parameter solution.

Seven parameters of 3D datum transformations can be used to relate two reference frames: three for translation, one for scale, and three for rotation. Using two sets of coordinates measured in two frames, these parameters can be solved using the Gauss–Markov (GM) model of least squares (LS) [2]. The assumption of the GM model is that there are no random errors in the coefficient matrix, but the observed coordinates of the reference station in the source coordinate system of the coefficient matrix have random errors; thus, the GM model cannot be used to describe the coordinate transformation problem accurately. For the case in which the coefficient matrix contains random errors, the error-in-variables (EIV) model can be used to describe the GM model, and the LS solution of the EIV model is called the total least squares (TLS).

In recent years, TLS has become a research topic of great interest in the field of geodesy and many algorithms have been developed and examined [3–6]. When the small rotation angle and scale are close to one, the datum transformation model can adopt the Bursa–Wolf model. Compared with classical LS, the accuracy of estimation results using TLS is greatly improved [7–10]. In the case of a large rotation angle and arbitrary scale, Felus et al. proposed an algorithm for a multiple EIV model [11]. Fang transformed the EIV model into a nonlinear Gauss–Markov model and proposed the 3D datum transformation algorithm under any rotation angle by taking the coordinates of common points in the source coordinate system as virtual observation values [12]. Chang and Li et al. proposed the analytical and closed-form solutions of 3D datum transformation, respectively [13, 14]. Because the rotation matrix of the datum transformation is a completely orthogonal matrix, there are strict orthogonal constraints. Fang proposed the universal constraint model of weighted TLS [5]. Lin et al. proposed the constraint solution of 3D datum transformation based on the nonlinear Gauss–Helmert model [15].

However, most TLS algorithms for datum transformation that focus on how to solve transformation parameters do not combine the two independent processes of transformation parameter estimation and noncommon station transformation; that is, noncommon station transformation is performed at the same time as the estimation of transformation parameters. In practice, there is a statistically significant correlation between the common and noncommon stations [16]; for example, the coordinates of common and noncommon stations come from the same control network adjustment results (e.g., GPS baseline network), but the existing model algorithm does not take into consideration the correlation between reference stations, so the estimation results cannot obtain the optimal solution in theory. To overcome this problem, Li et al. [17, 18] proposed the concept of seamless frame datum transformation, which combines the estimation parameters and coordinate transformation of noncommon stations. Compared with the traditional model, this transformation effectively improves the accuracy of the transformation coordinates. Wang et al. proposed the estimation model of 3D datum transformation under a large rotation angle and arbitrary scale conditions based on the generalized EIV model [19]. Lin et al. proposed the prediction model of 3D datum transformation of source coordinates in the form of geodetic coordinates based on the nonlinear Gauss–Helmert model [20].

Most of the current literature mainly concentrates on the datum transformation between two frames. When multiple (two or more) frames are involved, the transformation between the multiple source frames and a target frame, as mentioned earlier, clearly can be used to convert each source frame in turn with the target frame. The advantage is that we can draw lessons from the existing research achievements of Helmert transformation between the two frames directly. However, the existing methods cannot obtain the optimal solution. In recent years, a few researchers have studied the problem of simultaneous Helmert transformation with multiple frames. For example, Han et al. and Aktug proposed the closed solutions of this problem from the perspectives of geometry and algebra, respectively [21, 22], but the solutions all lack statistical optimality; in other words, the solutions are not LS.

The parameter estimation results of TLS are seriously affected when the observation of source frames contains gross errors. Mahboub et al. proposed a method of robust TLS based on selecting weight iteration for the EIV model [23]. Lu et al. and Tao et al. studied the robust TLS (RTLS) algorithm for 3D datum transformation and GPS height fitting, respectively, based on the Gauss–Helmert model [24, 25]. Jin et al. and Zhao et al. studied the total minimum L1 norm estimation method, taking into account the error of all variables [26, 27]. Wang et al. proposed the antidifference solution of weighted TLS (WTLS) by standardizing the residual to construct the equal-weight function and using the median method [6]. To solve the problem of processing outliers in universal 3D symmetrical Helmert transformation (probably with large rotation angles), Chang et al. derived the M-estimator by introducing the reweighted LS scheme [28]; in addition, the data snooping procedure was extended to the generalized EIV model by Wang et al. [29], consequently solving this problem by taking another approach.

Continuing from the analysis given above, we propose a robust predicted estimation for multiframe transformation, which constructs the weight factor function with standardized residuals and uses the median method to obtain the unit weight mean error. We need to consider the random errors of all observations and their correlation to finally achieve multiframe total transformation based on the generalized EIV model.

2. Extrapolation Estimation Method Based on the Generalized EIV Model

The function model for the extrapolation estimation method based on the generalized EIV model [19, 20] is as follows:

$$\boldsymbol{L}_1 - \boldsymbol{e}_{\boldsymbol{L}_1} = f\left(\boldsymbol{a}_1 - \boldsymbol{e}_{\boldsymbol{a}_1}, \boldsymbol{\xi}\right) \tag{1}$$

$$\overline{\boldsymbol{L}}_2 = f\left(\boldsymbol{a}_2 - \boldsymbol{e}_{\boldsymbol{a}_2}, \boldsymbol{\xi}\right), \tag{2}$$

where the n × 1 vector $\boldsymbol{L}_1$ denotes measurements and $\boldsymbol{e}_{\boldsymbol{L}_1}$ is the corresponding measurement error; the m × 1 vector $\overline{\boldsymbol{L}}_2$ denotes estimated values; the n × 1 vector $\boldsymbol{a}_1$ and m × 1 vector $\boldsymbol{a}_2$ are the measurements of the common and noncommon points, respectively, in the old frame; $\boldsymbol{e}_{\boldsymbol{a}_1}$ and $\boldsymbol{e}_{\boldsymbol{a}_2}$ are the corresponding measurement errors; $\boldsymbol{\xi}$ is the t × 1 vector of estimated parameters; and f is an abstract function.

The corresponding stochastic model can be described as

$$\boldsymbol{e} \sim N\left(0, \sigma_0^2 \mathbf{Q}\right) \tag{3}$$

$$\boldsymbol{e} = \begin{bmatrix} \boldsymbol{e}_{\boldsymbol{L}_1} \\ \boldsymbol{e}_{\boldsymbol{a}_1} \\ \boldsymbol{e}_{\boldsymbol{a}_2} \end{bmatrix}, \quad \mathbf{Q} = \begin{bmatrix} \mathbf{Q}_{\boldsymbol{L}_1\boldsymbol{L}_1} & \mathbf{Q}_{\boldsymbol{L}_1\boldsymbol{a}_1} & \mathbf{Q}_{\boldsymbol{L}_1\boldsymbol{a}_2} \\ \mathbf{Q}_{\boldsymbol{a}_1\boldsymbol{L}_1} & \mathbf{Q}_{\boldsymbol{a}_1\boldsymbol{a}_1} & \mathbf{Q}_{\boldsymbol{a}_1\boldsymbol{a}_2} \\ \mathbf{Q}_{\boldsymbol{a}_2\boldsymbol{L}_1} & \mathbf{Q}_{\boldsymbol{a}_2\boldsymbol{a}_1} & \mathbf{Q}_{\boldsymbol{a}_2\boldsymbol{a}_2} \end{bmatrix}, \tag{4}$$

where $\boldsymbol{Q}_{\boldsymbol{L}_1\boldsymbol{L}_1}$,$\boldsymbol{Q}_{\boldsymbol{a}_1\boldsymbol{a}_1}$, and $\boldsymbol{Q}_{\boldsymbol{a}_2\boldsymbol{a}_2}$ are the cofactor matrices of $\boldsymbol{L}_1$, $\boldsymbol{a}_1$, and $\boldsymbol{a}_2$, respectively; $\boldsymbol{Q}_{\boldsymbol{a}_1\boldsymbol{L}_1}$, $\boldsymbol{Q}_{\boldsymbol{a}_2\boldsymbol{L}_1}$, and $\boldsymbol{Q}_{\boldsymbol{a}_2\boldsymbol{a}_1}$ are the intercofactor matrices of $\boldsymbol{L}_1$, $\boldsymbol{a}_1$, and $\boldsymbol{a}_2$, respectively.

Taylor series expansion is applied to the right-hand side of (1) and (2) at the approximate values $\boldsymbol{\xi}^0$, $\boldsymbol{e}^0_{\boldsymbol{a}_1}$, and $\boldsymbol{e}^0_{\boldsymbol{a}_2}$ of $\boldsymbol{\xi}$, $\boldsymbol{e}_{\boldsymbol{a}_1}$, and $\boldsymbol{e}_{\boldsymbol{a}_2}$, respectively. Thus, (1) and (2) are now expressed as

$$\boldsymbol{L}_1 - \boldsymbol{e}_{\boldsymbol{L}_1} = f\left(\boldsymbol{a}_1 - \boldsymbol{e}^0_{\boldsymbol{a}_1}, \boldsymbol{\xi}^0\right) + \boldsymbol{A}_1 \mathrm{d}\boldsymbol{\xi} + \boldsymbol{B}_1\left(\boldsymbol{e}_{\boldsymbol{a}_1} - \boldsymbol{e}^0_{\boldsymbol{a}_1}\right) \quad (5)$$

$$\overline{\boldsymbol{L}}^0_2 + \mathrm{d}\overline{\boldsymbol{L}}_2 = f\left(\boldsymbol{a}_2 - \boldsymbol{e}^0_{\boldsymbol{a}_2}, \boldsymbol{\xi}^0\right) + \boldsymbol{A}_2 \mathrm{d}\boldsymbol{\xi} + \boldsymbol{B}_2\left(\boldsymbol{e}_{\boldsymbol{a}_2} - \boldsymbol{e}^0_{\boldsymbol{a}_2}\right), \quad (6)$$

where $\mathrm{d}\boldsymbol{\xi}$ denotes the correction vector of parameters, $\mathrm{d}\boldsymbol{\xi} = \boldsymbol{\xi} - \boldsymbol{\xi}^0$,

$$\begin{aligned}\boldsymbol{A}_1 &= \left.\frac{\partial f}{\partial \boldsymbol{\xi}^{\mathrm{T}}}\right| \left(\boldsymbol{e}^0_{\boldsymbol{a}_1}, \boldsymbol{\xi}^0\right),\\ \boldsymbol{B}_1 &= \left.\frac{\partial f}{\partial \boldsymbol{e}^{\mathrm{T}}_{\boldsymbol{a}_1}}\right| \left(\boldsymbol{e}^0_{\boldsymbol{a}_1}, \boldsymbol{\xi}^0\right),\\ \boldsymbol{A}_2 &= \left.\frac{\partial f}{\partial \boldsymbol{\xi}^{\mathrm{T}}}\right| \left(\boldsymbol{e}^0_{\boldsymbol{a}_2}, \boldsymbol{\xi}^0\right),\\ \boldsymbol{B}_2 &= \left.\frac{\partial f}{\partial \boldsymbol{e}^{\mathrm{T}}_{\boldsymbol{a}_2}}\right| \left(\boldsymbol{e}^0_{\boldsymbol{a}_2}, \boldsymbol{\xi}^0\right).\end{aligned} \quad (7)$$

Then the standard LS form of (5) and (6) is described as follows:

$$\boldsymbol{l} - \boldsymbol{G}\boldsymbol{e} = \boldsymbol{A}\mathrm{d}\boldsymbol{\theta} \quad (8)$$

where $\boldsymbol{l} = \begin{bmatrix} \boldsymbol{L}_1 - f(\boldsymbol{a}_1 - \boldsymbol{e}^0_{\boldsymbol{a}_1}, \boldsymbol{\xi}^0) + \boldsymbol{B}_1\boldsymbol{e}^0_{\boldsymbol{a}_1} \\ \overline{\boldsymbol{L}}^0_2 - f(\boldsymbol{a}_2 - \boldsymbol{e}^0_{\boldsymbol{a}_2}, \boldsymbol{\xi}^0) + \boldsymbol{B}_2\boldsymbol{e}^0_{\boldsymbol{a}_2}\end{bmatrix}$, $\boldsymbol{G} = \begin{bmatrix} \boldsymbol{I}_3 & \boldsymbol{B}_1 & 0 \\ 0 & 0 & \boldsymbol{B}_2 \end{bmatrix}$, $\boldsymbol{A} = \begin{bmatrix} \boldsymbol{A}_1 & 0 \\ \boldsymbol{A}_2 & -\boldsymbol{I}_m \end{bmatrix}$, $\mathrm{d}\boldsymbol{\theta} = \begin{bmatrix} \mathrm{d}\xi \\ \mathrm{d}\overline{L}_2 \end{bmatrix}$.

On the basis of the weighted LS error criterion, the LS solutions of the parameters and the estimation of the error vector can be calculated using (8):

$$\mathrm{d}\widehat{\boldsymbol{\theta}} = \left(\boldsymbol{A}^T \boldsymbol{Q}^{-1}_{\boldsymbol{G}} \boldsymbol{A}\right)^{-1} \boldsymbol{A}^T \boldsymbol{Q}^{-1}_{\boldsymbol{G}} \boldsymbol{l} \quad (9)$$

$$\widehat{\boldsymbol{e}} = \boldsymbol{Q}\boldsymbol{G}^{\mathrm{T}} \boldsymbol{Q}^{-1}_{\boldsymbol{G}} \left(\boldsymbol{l} - \boldsymbol{A}\mathrm{d}\widehat{\boldsymbol{\theta}}\right), \quad (10)$$

where $\boldsymbol{Q}_{\boldsymbol{G}} = \boldsymbol{G}\boldsymbol{Q}\boldsymbol{G}^{\mathrm{T}}$.

3. Robust Estimation Method Based on the Standardized Residuals and Median

The accurate estimated parameters are difficult to obtain using (8) if there are gross errors in the observation vector or coefficient matrix $\boldsymbol{A}$. For this, we propose a robust prediction algorithm based on the generalized EIV model. We use the robust estimation introduced by Wang et al. [6]; it is based on the standardized residuals and median robust model. The robust prediction model is more reasonable in theory than the existing TLS robust methods and has two advantages: the weight factor function constructed by the standardized residuals can take into account the robustness of both the observation space and structure space; the estimation of the unit weight mean error obtained by the median method has greater robustness in the iterative process. The estimation criterion of the robust prediction algorithm is described as follows:

$$\boldsymbol{e}^{\mathrm{T}} \overline{\boldsymbol{Q}}^{-1} \boldsymbol{e} = \min, \quad (11)$$

where

$$\overline{\boldsymbol{Q}} = \begin{bmatrix} \overline{\boldsymbol{Q}}_{\boldsymbol{L}_1\boldsymbol{L}_1} & \overline{\boldsymbol{Q}}_{\boldsymbol{L}_1\boldsymbol{a}_1} & \overline{\boldsymbol{Q}}_{\boldsymbol{L}_1\boldsymbol{a}_2} \\ \overline{\boldsymbol{Q}}_{\boldsymbol{a}_1\boldsymbol{L}_1} & \overline{\boldsymbol{Q}}_{\boldsymbol{a}_1\boldsymbol{a}_1} & \overline{\boldsymbol{Q}}_{\boldsymbol{a}_1\boldsymbol{a}_2} \\ \overline{\boldsymbol{Q}}_{\boldsymbol{a}_2\boldsymbol{L}_1} & \overline{\boldsymbol{Q}}_{\boldsymbol{a}_2\boldsymbol{a}_1} & \overline{\boldsymbol{Q}}_{\boldsymbol{a}_2\boldsymbol{a}_2} \end{bmatrix} = \overline{\boldsymbol{P}}^{-1}, \quad (12)$$

where $\overline{\boldsymbol{Q}}_{\boldsymbol{L}_1\boldsymbol{L}_1}$, $\overline{\boldsymbol{Q}}_{\boldsymbol{a}_1\boldsymbol{a}_1}$, and $\overline{\boldsymbol{Q}}_{\boldsymbol{a}_2\boldsymbol{a}_2}$ are the equivalent cofactor matrices of observation vectors $\boldsymbol{L}_1$, $\boldsymbol{a}_1$, and $\boldsymbol{a}_2$, respectively; $\overline{\boldsymbol{Q}}_{\boldsymbol{a}_1\boldsymbol{L}_1}$, $\overline{\boldsymbol{Q}}_{\boldsymbol{a}_2\boldsymbol{L}_1}$, and $\overline{\boldsymbol{Q}}_{\boldsymbol{a}_2\boldsymbol{a}_1}$ are the equivalent intercofactor matrices of observation vectors $\boldsymbol{L}_1$, $\boldsymbol{a}_1$, and $\boldsymbol{a}_2$, respectively.

Then, the solutions of the parameters and the estimation of the error vector are as follows:

$$\mathrm{d}\widehat{\boldsymbol{\theta}} = \left(\boldsymbol{A}^T \overline{\boldsymbol{Q}}^{-1}_{\boldsymbol{G}} \boldsymbol{A}\right)^{-1} \boldsymbol{A}^T \overline{\boldsymbol{Q}}^{-1}_{\boldsymbol{G}} \boldsymbol{l} \quad (13)$$

$$\widehat{\boldsymbol{e}} = \overline{\boldsymbol{Q}}\boldsymbol{G}^{\mathrm{T}} \overline{\boldsymbol{Q}}^{-1}_{\boldsymbol{G}} \left(\boldsymbol{l} - \boldsymbol{A}\mathrm{d}\widehat{\boldsymbol{\theta}}\right). \quad (14)$$

Because the correlation between the observations is taken into account in the stochastic model of the extrapolation estimation method, it is necessary to construct the equivalent cofactor matrices in the form of double factors as follows [6, 30]:

$$\overline{q}_i = q_i R_{ii} \quad (15a)$$

$$\overline{q}_{ij} = q_{ij} \sqrt{R_{ii}} \sqrt{R_{jj}}, \quad (15b)$$

where the subscripts i and j represent the serial numbers of the observed values; q_i and q_{ij} denote the elements in cofactor matrix Q; $\overline{q}_{ij}$ and $\overline{q}_{ij}$ denote the elements in equivalent cofactor matrix $\overline{\boldsymbol{Q}}$; and R_{ii} and R_{jj} are the reciprocals of the weight factors, which are called the cofactor factors [30]. Additionally, because the generalized EIV model is adopted in this paper, the prior information is directly the weight matrix/cofactor matrix of the observation vector, and there is no weight reduction problem of the standard EIV for the fixed elements of the coefficient matrix.

The corresponding cofactor factor function can be obtained by inverting the IGGIII weight factor function as follows.

$$R_{ii} = \begin{cases} 1.0 & \left|\widetilde{e}_i\right| \le k_0 \\ \dfrac{\left|\widetilde{e}_i\right|}{k_0}\left(\dfrac{k_1 - k_0}{k_1 - \left|\widetilde{e}_i\right|}\right)^2 & k_0 < \left|\widetilde{e}_i\right| \le k_1 \\ 10^{30} & k_1 < \left|\widetilde{e}_i\right| \end{cases} \quad (16)$$

It should be noted that the theoretical value of the corresponding cofactor should be infinite because the weight factor of the third line in (16) is zero. However, to facilitate calculation, a large number is used to satisfy the requirement in the numerical calculation, and the abnormal observation information has little effect on parameter estimation.

Because of the accuracy difference between variables, the cofactors are calculated with standardized residual $\tilde{e}_i$ to guarantee the antierror effect. The formula of the standardized residual $\tilde{e}_i$ is as follows:

$$\tilde{e}_i = \frac{\hat{e}_i}{\sigma_0 \sqrt{\mathbf{Q}_{e_i}}}, \tag{17}$$

where $\hat{e}_i$ is the ith element of residual vector $\hat{\boldsymbol{e}}$, $\mathbf{Q}_{e_i}$ is the cofactor of $\hat{e}_i$, and σ_0 is the standard error of unit weight, which is expressed as follows:

$$\sigma_0 = 1.4826 \times \underset{i=1}{\overset{n}{med}} \left(\left| \frac{e_i}{\sqrt{\mathbf{Q}_{e_i}}} \right| \right). \tag{18}$$

According to the law of cofactor propagation, we can easily obtain cofactor matrices $\mathbf{Q}_e$ of residual errors; see Wang et al. [6] for the detailed derivation process. Therefore, cofactor matrices $\mathbf{Q}_e$ can be estimated as

$$\mathbf{Q}_e = \boldsymbol{M}\mathbf{Q}_{\boldsymbol{R}}\boldsymbol{M}^{\mathrm{T}}, \tag{19}$$

where $\mathbf{Q}_{\boldsymbol{R}} = \mathbf{Q}_{\boldsymbol{G}} - \boldsymbol{A}(\boldsymbol{A}^T\mathbf{Q}_{\boldsymbol{G}}^{-1}\boldsymbol{A})^{-1}\boldsymbol{A}^T$ and $\boldsymbol{M} = \mathbf{Q}\boldsymbol{G}^{\mathrm{T}}\mathbf{Q}_{\boldsymbol{G}}^{-1}$.

It should be pointed out that if the number of redundancies is low, outliers would significantly affect the residuals of normal observations and the observation with larger residuals may not contain outliers. In other words, almost all methods that process outliers will break down when there are only a few redundant observations.

4. Robust Prediction Algorithms for Multiframe Transformation

Without loss of generality, in this paper, we consider the transformation between two source frames and one target frame. The two source frames are called the first and second source frames. Assume the following four observation datasets: (i) the common stations of three frames $\Pi_1 = [1, 2, \ldots, m_1]$; (ii) the common stations of the first and second source frames $\Pi_2 = [1, 2, \ldots, m_2]$; (iii) the noncommon stations of the first source frame $\Pi_3 = [1, 2, \ldots, m_3]$; and (iv) the noncommon stations of the second source frame $\Pi_4 = [1, 2, \ldots, m_4]$. The terms $\boldsymbol{X}, \boldsymbol{Y}, \boldsymbol{Z}$, and $\boldsymbol{W}$ are used to represent the 3D coordinate vectors of the common stations in the above four observation datasets, respectively. Considering the first dataset as an example, $\boldsymbol{X}$, $\boldsymbol{X}'$, and $\boldsymbol{X}''$ denote the 3D coordinate vectors of the target frame, first source frame, and second source frame, respectively. The observation or estimation equations with respect to the ith element in each dataset can be expressed as

$$\begin{aligned} \boldsymbol{X}_i - \boldsymbol{e}_{\boldsymbol{X}_i} &= \boldsymbol{t}_1 + s_1\boldsymbol{R}_1\left(\boldsymbol{X}_i' - \boldsymbol{e}_{\boldsymbol{X}_i'}\right) \\ \boldsymbol{X}_i - \boldsymbol{e}_{\boldsymbol{X}_i} &= \boldsymbol{t}_2 + s_2\boldsymbol{R}_2\left(\boldsymbol{X}_i'' - \boldsymbol{e}_{\boldsymbol{X}_i''}\right) \end{aligned} \tag{20}$$

$$\begin{aligned} \overline{\boldsymbol{Y}}_i &= \boldsymbol{t}_1 + s_1\boldsymbol{R}_1\left(\boldsymbol{Y}_i' - \boldsymbol{e}_{\boldsymbol{Y}_i'}\right) \\ \overline{\boldsymbol{Y}}_i &= \boldsymbol{t}_2 + s_2\boldsymbol{R}_2\left(\boldsymbol{Y}_i'' - \boldsymbol{e}_{\boldsymbol{Y}_i''}\right) \\ \overline{\boldsymbol{Z}}_i &= \boldsymbol{t}_1 + s_1\boldsymbol{R}_1\left(\boldsymbol{Z}_i' - \boldsymbol{e}_{\boldsymbol{Z}_i'}\right) \\ \overline{\boldsymbol{W}}_i &= \boldsymbol{t}_2 + s_2\boldsymbol{R}_2\left(\boldsymbol{W}_i'' - \boldsymbol{e}_{\boldsymbol{W}_i''}\right) \end{aligned} \tag{21}$$

where e denotes the error vector that corresponds to the coordinate observation vector; $\boldsymbol{t}_1$ and $\boldsymbol{t}_2$ are the 3×1 translation parameters between the first source frame or second source frame and the target frame, respectively; s_1 and s_2 are the scale parameters between the first source frame or second source frame and the target frame, respectively; and R_1 and R_2 are the 3×3 rotation matrices between the first source frame or second source frame and the target frame, respectively, and can be described as follows:

$$\begin{aligned} \boldsymbol{R}_1 &= \boldsymbol{R}(\gamma_1)\,\boldsymbol{R}(\beta_1)\,\boldsymbol{R}(\alpha_1), \\ \boldsymbol{R}_2 &= \boldsymbol{R}(\gamma_2)\,\boldsymbol{R}(\beta_2)\,\boldsymbol{R}(\alpha_2) \end{aligned} \tag{22}$$

$$\begin{aligned} \boldsymbol{R}(\alpha) &= \begin{bmatrix} 1 & 0 & 0 \\ 0 & \cos\alpha & \sin\alpha \\ 0 & -\sin\alpha & \cos\alpha \end{bmatrix}; \\ \boldsymbol{R}(\beta) &= \begin{bmatrix} \cos\beta & 0 & -\sin\beta \\ 0 & 1 & 0 \\ \sin\beta & 0 & \cos\beta \end{bmatrix}; \\ \boldsymbol{R}(\gamma) &= \begin{bmatrix} \cos\gamma & \sin\gamma & 0 \\ -\sin\gamma & \cos\gamma & 0 \\ 0 & 0 & 1 \end{bmatrix}, \end{aligned} \tag{23}$$

where α_1, β_1, and γ_1 are the rotation parameters between the first source frame and the target frame; α_2, β_2, and γ_2 are the rotation parameters between the second source frame and the target frame.

The corresponding random model is as follows:

$$\boldsymbol{e} \sim N\left(0, \sigma_0^2\mathbf{Q}\right) \tag{24}$$

$$\boldsymbol{e} = \left[\boldsymbol{e}_{\boldsymbol{X}}^{\mathrm{T}} \ \boldsymbol{e}_{\boldsymbol{X}'}^{\mathrm{T}} \ \boldsymbol{e}_{\boldsymbol{X}''}^{\mathrm{T}} \ \boldsymbol{e}_{\boldsymbol{Y}'}^{\mathrm{T}} \ \boldsymbol{e}_{\boldsymbol{Y}''}^{\mathrm{T}} \ \boldsymbol{e}_{\boldsymbol{Z}'}^{\mathrm{T}} \ \boldsymbol{e}_{\boldsymbol{W}''}^{\mathrm{T}}\right]^{\mathrm{T}} \tag{25}$$

$$\mathbf{Q} = \begin{bmatrix} \mathbf{Q}_{XX} & 0 & 0 & 0 & 0 & 0 & 0 \\ 0 & \mathbf{Q}_{X'X'} & \mathbf{Q}_{X'Y'} & \mathbf{Q}_{X'Z'} & 0 & 0 & 0 \\ 0 & \mathbf{Q}_{Y'X'} & \mathbf{Q}_{Y'Y'} & \mathbf{Q}_{Y'Z'} & 0 & 0 & 0 \\ 0 & \mathbf{Q}_{Z'X'} & \mathbf{Q}_{Z'Y'} & \mathbf{Q}_{Z'Z'} & 0 & 0 & 0 \\ 0 & 0 & 0 & 0 & \mathbf{Q}_{X''X''} & \mathbf{Q}_{X''Y''} & \mathbf{Q}_{X''W''} \\ 0 & 0 & 0 & 0 & \mathbf{Q}_{Y''X''} & \mathbf{Q}_{Y''Y''} & \mathbf{Q}_{Y''W''} \\ 0 & 0 & 0 & 0 & \mathbf{Q}_{W''X''} & \mathbf{Q}_{W''Y''} & \mathbf{Q}_{W''W''} \end{bmatrix}. \tag{26}$$

In a similar manner, (20) and (21) are expanded using the Taylor series expansion method. Then,

$$\begin{aligned}
\boldsymbol{L}_{1i}-\boldsymbol{e}_{\boldsymbol{X}_i}+s_1^0\boldsymbol{R}_1^0\boldsymbol{e}_{\boldsymbol{X}_i'}&=\boldsymbol{A}_{1,j}\mathrm{d}\boldsymbol{\xi}_1\\
\boldsymbol{L}_{2i}-\boldsymbol{e}_{\boldsymbol{X}_i}+s_2^0\boldsymbol{R}_2^0\boldsymbol{e}_{\boldsymbol{X}_i''}&=\boldsymbol{A}_{2,j}\mathrm{d}\boldsymbol{\xi}_2\\
\boldsymbol{L}_{3i}+s_1^0\boldsymbol{R}_1^0\boldsymbol{e}_{\boldsymbol{Y}_i'}&=\boldsymbol{A}_{3,j}\mathrm{d}\boldsymbol{\xi}_1-\mathrm{d}\overline{\boldsymbol{Y}}_i\\
\boldsymbol{L}_{4i}+s_2^0\boldsymbol{R}_2^0\boldsymbol{e}_{\boldsymbol{Y}_i''}&=\boldsymbol{A}_{4,j}\mathrm{d}\boldsymbol{\xi}_2-\mathrm{d}\overline{\boldsymbol{Y}}_i\\
\boldsymbol{L}_{5i}+s_1^0\boldsymbol{R}_1^0\boldsymbol{e}_{\boldsymbol{Z}_i'}&=\boldsymbol{A}_{5,j}\mathrm{d}\boldsymbol{\xi}_1-\mathrm{d}\overline{\boldsymbol{Z}}_i\\
\boldsymbol{L}_{6i}+s_2^0\boldsymbol{R}_2^0\boldsymbol{e}_{\boldsymbol{W}_i''}&=\boldsymbol{A}_{6,j}\mathrm{d}\boldsymbol{\xi}_2-\mathrm{d}\overline{\boldsymbol{W}}_i
\end{aligned}\tag{27}$$

where

$$\begin{aligned}
\boldsymbol{L}_{1i}&=\boldsymbol{X}_i-\boldsymbol{t}_1^0-s_1^0\boldsymbol{R}_1^0\boldsymbol{X}_i{}',\\
\boldsymbol{L}_{2i}&=\boldsymbol{X}_i-\boldsymbol{t}_2^0-s_2^0\boldsymbol{R}_2^0\boldsymbol{X}_i{}'',\\
\boldsymbol{L}_{3i}&=\boldsymbol{Y}_i^0-\boldsymbol{t}_1^0-s_1^0\boldsymbol{R}_1^0\boldsymbol{Y}_i{}',\\
\boldsymbol{L}_{4i}&=\boldsymbol{Y}_i^0-\boldsymbol{t}_2^0-s_2^0\boldsymbol{R}_2^0\boldsymbol{Y}_i{}'',\\
\boldsymbol{L}_{5i}&=\boldsymbol{Z}_i^0-\boldsymbol{t}_1^0-s_1^0\boldsymbol{R}_1^0\boldsymbol{Z}_i{}',\\
\boldsymbol{L}_{6i}&=\boldsymbol{W}_i^0-\boldsymbol{t}_2^0-s_2^0\boldsymbol{R}_2^0\boldsymbol{W}_i{}''\\
\boldsymbol{A}_{1,j}&=\left[\boldsymbol{I}_3\;\;\boldsymbol{R}_1^0\left(\boldsymbol{X}_i'-\boldsymbol{e}_{\boldsymbol{X}_i'}^0\right)\;\;s_1^0\frac{\delta\boldsymbol{R}_1}{\delta\alpha_1}\left(\boldsymbol{X}_i'-\boldsymbol{e}_{\boldsymbol{X}_i'}^0\right)\;\;s_1^0\frac{\delta\boldsymbol{R}_1}{\delta\beta_1}\left(\boldsymbol{X}_i'-\boldsymbol{e}_{\boldsymbol{X}_i'}^0\right)\;\;s_1^0\frac{\delta\boldsymbol{R}_1}{\delta\gamma_1}\left(\boldsymbol{X}_i'-\boldsymbol{e}_{\boldsymbol{X}_i'}^0\right)\right],\\
\boldsymbol{A}_{2,j}&=\left[\boldsymbol{I}_3\;\;\boldsymbol{R}_2^0\left(\boldsymbol{X}_i''-\boldsymbol{e}_{\boldsymbol{X}_i''}^0\right)\;\;s_2^0\frac{\delta\boldsymbol{R}_2}{\delta\alpha_2}\left(\boldsymbol{X}_i''-\boldsymbol{e}_{\boldsymbol{X}_i''}^0\right)\;\;s_2^0\frac{\delta\boldsymbol{R}_2}{\delta\beta_2}\left(\boldsymbol{X}_i''-\boldsymbol{e}_{\boldsymbol{X}_i''}^0\right)\;\;s_2^0\frac{\delta\boldsymbol{R}_2}{\delta\gamma_2}\left(\boldsymbol{X}_i''-\boldsymbol{e}_{\boldsymbol{X}_i''}^0\right)\right],\\
\frac{\delta\boldsymbol{R}}{\delta\alpha}&=\boldsymbol{R}(\gamma)\boldsymbol{R}(\beta)\frac{\delta\boldsymbol{R}(\alpha)}{\delta\alpha},\\
\frac{\delta\boldsymbol{R}}{\delta\alpha}&=\boldsymbol{R}(\gamma)\frac{\delta\boldsymbol{R}(\beta)}{\delta\beta}\boldsymbol{R}(\alpha),\\
\frac{\delta\boldsymbol{R}}{\delta\alpha}&=\frac{\delta\boldsymbol{R}(\gamma)}{\delta\gamma}\boldsymbol{R}(\beta)\boldsymbol{R}(\alpha),\\
\frac{\delta\boldsymbol{R}(\alpha)}{\delta\alpha}&=\begin{bmatrix}0&0&0\\0&-\sin\alpha&\cos\alpha\\0&-\cos\alpha&-\sin\alpha\end{bmatrix},\\
\frac{\delta\boldsymbol{R}(\beta)}{\delta\beta}&=\begin{bmatrix}-\sin\beta&0&-\cos\beta\\0&0&0\\\cos\beta&0&-\sin\beta\end{bmatrix},\\
\frac{\delta\boldsymbol{R}(\gamma)}{\delta\gamma}&=\begin{bmatrix}-\sin\gamma&\cos\gamma&0\\-\cos\gamma&-\sin\gamma&0\\0&0&0\end{bmatrix},
\end{aligned}\tag{28}$$

where the format of $\boldsymbol{A}_{3,j}$ and $\boldsymbol{A}_{5,j}$ is the same as that of $\boldsymbol{A}_{1,j}$; the format of $\boldsymbol{A}_{4,j}$ and $\boldsymbol{A}_{6,j}$ is the same as that of $\boldsymbol{A}_{2,j}$.

All observations can be linked to obtain

$$\begin{aligned}
\boldsymbol{L}_1-\boldsymbol{e}_{\boldsymbol{X}}+\boldsymbol{B}_1\boldsymbol{e}_{\boldsymbol{X}_i'}&=\boldsymbol{A}_1\mathrm{d}\boldsymbol{\xi}_1\\
\boldsymbol{L}_2-\boldsymbol{e}_{\boldsymbol{X}}+\boldsymbol{B}_2\boldsymbol{e}_{\boldsymbol{X}_i''}&=\boldsymbol{A}_2\mathrm{d}\boldsymbol{\xi}_2\\
\boldsymbol{L}_3+\boldsymbol{B}_3\boldsymbol{e}_{\boldsymbol{Y}'}&=\boldsymbol{A}_3\mathrm{d}\boldsymbol{\xi}_1-\mathrm{d}\overline{\boldsymbol{Y}}\\
\boldsymbol{L}_4+\boldsymbol{B}_4\boldsymbol{e}_{\boldsymbol{Y}''}&=\boldsymbol{A}_4\mathrm{d}\boldsymbol{\xi}_2-\mathrm{d}\overline{\boldsymbol{Y}}\\
\boldsymbol{L}_5+\boldsymbol{B}_5\boldsymbol{e}_{\boldsymbol{Z}'}&=\boldsymbol{A}_5\mathrm{d}\boldsymbol{\xi}_1-\mathrm{d}\overline{\boldsymbol{Z}}\\
\boldsymbol{L}_6+\boldsymbol{B}_6\boldsymbol{e}_{\boldsymbol{W}''}&=\boldsymbol{A}_6\mathrm{d}\boldsymbol{\xi}_2-\mathrm{d}\overline{\boldsymbol{W}}
\end{aligned}\tag{29}$$

where

$$
\begin{aligned}
\boldsymbol{L}_1 &= \left[\boldsymbol{L}_{1,1}^{\mathrm{T}} \ \ \boldsymbol{L}_{1,2}^{\mathrm{T}} \ \ \cdots \ \ \boldsymbol{L}_{1,m_1}^{\mathrm{T}}\right]^{\mathrm{T}}, \\
\boldsymbol{L}_2 &= \left[\boldsymbol{L}_{2,1}^{\mathrm{T}} \ \ \boldsymbol{L}_{2,2}^{\mathrm{T}} \ \ \cdots \ \ \boldsymbol{L}_{2,m_1}^{\mathrm{T}}\right]^{\mathrm{T}}, \\
\boldsymbol{L}_3 &= \left[\boldsymbol{L}_{3,1}^{\mathrm{T}} \ \ \boldsymbol{L}_{3,2}^{\mathrm{T}} \ \ \cdots \ \ \boldsymbol{L}_{3,m_2}^{\mathrm{T}}\right]^{\mathrm{T}}, \\
\boldsymbol{L}_4 &= \left[\boldsymbol{L}_{4,1}^{\mathrm{T}} \ \ \boldsymbol{L}_{4,2}^{\mathrm{T}} \ \ \cdots \ \ \boldsymbol{L}_{4,m_2}^{\mathrm{T}}\right]^{\mathrm{T}}, \\
\boldsymbol{L}_5 &= \left[\boldsymbol{L}_{5,1}^{\mathrm{T}} \ \ \boldsymbol{L}_{5,2}^{\mathrm{T}} \ \ \cdots \ \ \boldsymbol{L}_{5,m_3}^{\mathrm{T}}\right]^{\mathrm{T}}, \\
\boldsymbol{L}_6 &= \left[\boldsymbol{L}_{6,1}^{\mathrm{T}} \ \ \boldsymbol{L}_{6,2}^{\mathrm{T}} \ \ \cdots \ \ \boldsymbol{L}_{6,m_4}^{\mathrm{T}}\right]^{\mathrm{T}}, \\
\boldsymbol{B}_1 &= s_1^0 \boldsymbol{R}_1^0 \otimes \boldsymbol{I}_{m_1}, \\
\boldsymbol{B}_2 &= s_2^0 \boldsymbol{R}_2^0 \otimes \boldsymbol{I}_{m_1}, \\
\boldsymbol{B}_3 &= s_1^0 \boldsymbol{R}_1^0 \otimes \boldsymbol{I}_{m_2}, \\
\boldsymbol{B}_4 &= s_2^0 \boldsymbol{R}_2^0 \otimes \boldsymbol{I}_{m_2}, \\
\boldsymbol{B}_5 &= s_1^0 \boldsymbol{R}_1^0 \otimes \boldsymbol{I}_{m_3}, \\
\boldsymbol{B}_6 &= s_2^0 \boldsymbol{R}_2^0 \otimes \boldsymbol{I}_{m_4}.
\end{aligned}
\tag{30}
$$

Then the standard LS form of (29) is described as follows:

$$\boldsymbol{l} - \boldsymbol{G}\boldsymbol{e} = \boldsymbol{A}\mathrm{d}\boldsymbol{\theta}, \tag{31}$$

where

$$
\begin{aligned}
\boldsymbol{A} &= \begin{bmatrix} \boldsymbol{A}_1 & 0 & 0 & 0 & 0 \\ 0 & \boldsymbol{A}_2 & 0 & 0 & 0 \\ \boldsymbol{A}_3 & 0 & -\boldsymbol{I}_{m_2} & 0 & 0 \\ 0 & \boldsymbol{A}_4 & -\boldsymbol{I}_{m_2} & 0 & 0 \\ \boldsymbol{A}_4 & 0 & 0 & -\boldsymbol{I}_{m_3} & 0 \\ 0 & \boldsymbol{A}_6 & 0 & 0 & -\boldsymbol{I}_{m_4} \end{bmatrix}, \\
\boldsymbol{G} &= \begin{bmatrix} \boldsymbol{I}_{m_1} & -\boldsymbol{B}_1 & 0 & 0 & 0 & 0 & 0 \\ \boldsymbol{I}_{m_1} & 0 & -\boldsymbol{B}_2 & 0 & 0 & 0 & 0 \\ 0 & 0 & 0 & -\boldsymbol{B}_3 & 0 & 0 & 0 \\ 0 & 0 & 0 & 0 & -\boldsymbol{B}_4 & 0 & 0 \\ 0 & 0 & 0 & 0 & 0 & -\boldsymbol{B}_5 & 0 \\ 0 & 0 & 0 & 0 & 0 & 0 & -\boldsymbol{B}_6 \end{bmatrix}, \\
\boldsymbol{l} &= \left[\boldsymbol{L}_1^{\mathrm{T}} \ \ \boldsymbol{L}_2^{\mathrm{T}} \ \ \boldsymbol{L}_3^{\mathrm{T}} \ \ \boldsymbol{L}_4^{\mathrm{T}} \ \ \boldsymbol{L}_5^{\mathrm{T}} \ \ \boldsymbol{L}_6^{\mathrm{T}}\right]^{\mathrm{T}}, \\
\mathrm{d}\boldsymbol{\theta} &= \left[\mathrm{d}\boldsymbol{\xi}_1^{\mathrm{T}} \ \ \mathrm{d}\boldsymbol{\xi}_2^{\mathrm{T}} \ \ \mathrm{d}\overline{\boldsymbol{Y}} \ \ \mathrm{d}\overline{\boldsymbol{Z}} \ \ \mathrm{d}\overline{\boldsymbol{W}}\right].
\end{aligned}
\tag{32}
$$

Following (26) and (31), the robust LS solution of (31) can be obtained using the robust prediction estimation method in the previous section.

5. Experimental Analysis

Assume that (i) the transformation parameters between the first source frame and the target frame are $\boldsymbol{t}_1 = [100 \ \ -99 \ \ 200]^{\mathrm{T}}$, $s_1 = 0.83$, $\alpha_1 = 0.45$, $\beta_1 = 0.37$, $\gamma_1 = 0.54$; (ii) the transformation parameters between the second source frame and the target frame are $\boldsymbol{t}_2 = [200 \ \ 120 \ \ -170]^{\mathrm{T}}$, $s_2 = 0.79$, $\alpha_2 = 0.23$, $\beta_2 = 0.48$, $\gamma_2 = 0.33$. The four dimensions of the corresponding observation datasets are $m_1 = 10$, $m_2 = 6$, $m_3 = 5$, and $m_4 = 4$, respectively.

Considering the WGS-84 frame as the target frame, the geodetic coordinates of the target frame, including the latitude, longitude, and geodetic height, which are randomly generated in the form of a uniform distribution within the ranges $[-\pi/2, \pi/2]$, $[-\pi, \pi]$, and $[10, \ 3000]$, are transformed into the corresponding 3D rectangular coordinates. The observation station coordinates of the first and second source frames are obtained from the true value of the given transformation parameters. The 3D distribution of the simulation data is shown in Figure 1.

The detailed procedures for generating covariance matrices of 10 observation stations in the target frame are as follows:

(1) Generate 30 diagonal matrices D, that is, the standard error, using uniform distribution U [0.03 m, 0.04 m].

(2) Generate 30×30 random matrix $\boldsymbol{M}$ using uniform distribution U [−0.8 0.8], $\boldsymbol{M} = \boldsymbol{T}_1\boldsymbol{T}_2$ using QR decomposition for M.

(3) Generate 10 covariance matrices of 10 observation stations in the target frame: $\boldsymbol{Q}_1 = \boldsymbol{T}_1\boldsymbol{D}\boldsymbol{T}_1^{\mathrm{T}}$.

The variance-covariance matrix generation process for the first source frame and second source frame is as above, with the uniform distributions being U[0.05 m, 0.7 m] and U[0.08 m, 0.1 m], respectively. The correlation coefficients are generated using uniform distribution U [−0.8, 0.8].

The truth values of the parameters and coordinates above are constant when the Monte Carlo experiment is run 1,000 times, but the measurement error of each experiment is generated independently using the variance-covariance matrices mentioned above with zero mean Gaussian distribution. Additionally, assume that the number of gross errors is three, the location of gross errors are randomly generated at the common stations, and the sizes are in the range (−30, −10) and (10, 30) times the prior standard error. Observation data with random errors are added each time.

Set the prior unit weight mean error to 0.01, and the calculation scheme is as follows:

Before the gross errors are added, three schemes are proposed: (1) the prediction estimation algorithm of the independent transformation between the first source frame and the target frame [19]; (2) the prediction estimation algorithm between the second source frame and the target frame; and (3) the prediction estimation multiframe total transformation algorithm proposed in this paper.

After the gross errors are added, four additional schemes are proposed: (4) the prediction estimation algorithm of the total transformation of the multiple frames proposed in this paper; (5) the robust prediction estimation algorithm between the first source frame and the target frame; (6) the

Table 1: Transformation parameter accuracies in terms of RMSE between the first source frame and the target frame.

Scheme	ΔX/m	ΔY/m	ΔZ/m	s/ppm	ε_x/mas	ε_y/mas	ε_z/mas
(1)	0.0262	0.0254	0.0242	0.0045	360.1	968.5	516.8
(3)	0.0244	0.0226	0.0217	0.0033	113.5	101.6	182.6
(4)	0.1343	0.1252	0.1038	0.1048	1265.3	1742.5	1683.7
(5)	0.0353	0.0398	0.0344	0.0078	432.4	1023.8	653.3
(7)	0.0268	0.0287	0.0259	0.0057	328.6	562.4	423.5

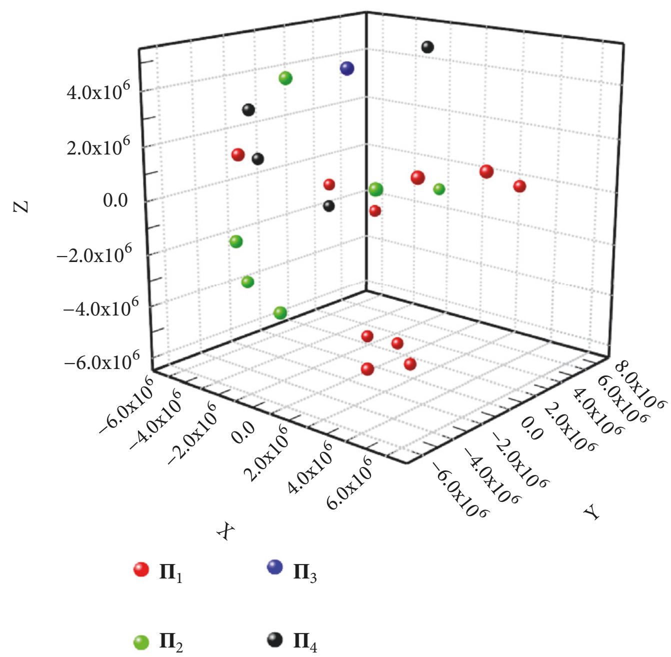

Figure 1: 3D distribution of observation stations.

robust prediction estimation algorithm between the second source frame and the target frame; and (7) the robust prediction estimation multiframe total transformation algorithm proposed in this paper.

According to the results of different schemes, the seven transformation parameters and the prediction points in the target frame are calculated with Root Mean Square (RMS) as the accuracy evaluation index, and the specific calculation formula is described as follows:

$$\sigma^2 = \sqrt{\frac{\sum_i^n \left(\hat{\delta} - \delta\right)}{n}}, \tag{33}$$

where $\hat{\delta}$ is the estimated value, δ is the true value, and n is the number of estimations.

From Tables 1 and 2 and Figures 1, 2, and 3, we can see the following:

(1) Before the gross errors are added, comparing the results from schemes 1, 2, and 3, the result of scheme 3 is optimal, and it lies not only in the transformation parameter estimation but also particularly in common stations of the two source frames (the observation set $\mathbf{\Pi}_2$). There are two transformation solutions for the same reference station in the target frame using schemes 1 and 2, as shown in Figure 2, so it is difficult to decide which one is the optimal solution. The multiframe unified transformation model avoids the problem of solution selection; in addition, unlike an independent transformation, it also takes into full account the existing information of two source frames; thus, the accuracy of the solution is improved.

(2) Figures 3 and 4 show the transformation results of the noncommon stations of a single source frame. Better transformation results are obtained because the multiframe transformation can improve the transformation accuracy.

(3) After the gross errors are added, a distortion of the estimated parameters often appears when the robust algorithm is not adopted, as in scheme 4. Compared with scheme 4, the robust estimation adopted in schemes 5, 6, and 7 results in different degrees of improvement. The total transformation model of multiple frames takes more existing information into account; that is, it has better spatial geometric distribution. Therefore, under the premise of adopting the same robust method, the robust prediction estimation algorithm (scheme 7), which adopts the total transformation of multiple frames, has the best performance and can obtain more accurate solutions than independent transformation.

(4) There are multiple advantages in taking the coordinates of the points to be converted in the target frame as

Table 2: Transformation parameter accuracies in terms of the RMSE between the second source frame and the target frame.

scheme	ΔX/m	ΔY/m	ΔZ/m	s/ppm	ε_x/mas	ε_y/mas	ε_z/mas
(2)	0.0455	0.0370	0.0381	0.0096	370.1	814.9	988.7
(3)	0.0365	0.0324	0.0323	0.0073	344.4	396.1	391.6
(4)	0.1562	0.1437	0.1517	0.1359	1472.2	1553.6	1842.4
(6)	0.0524	0.0418	0.0437	0.0103	417.6	931.2	1024.3
(7)	0.0393	0.0361	0.0376	0.0087	382.3	448.7	512.8

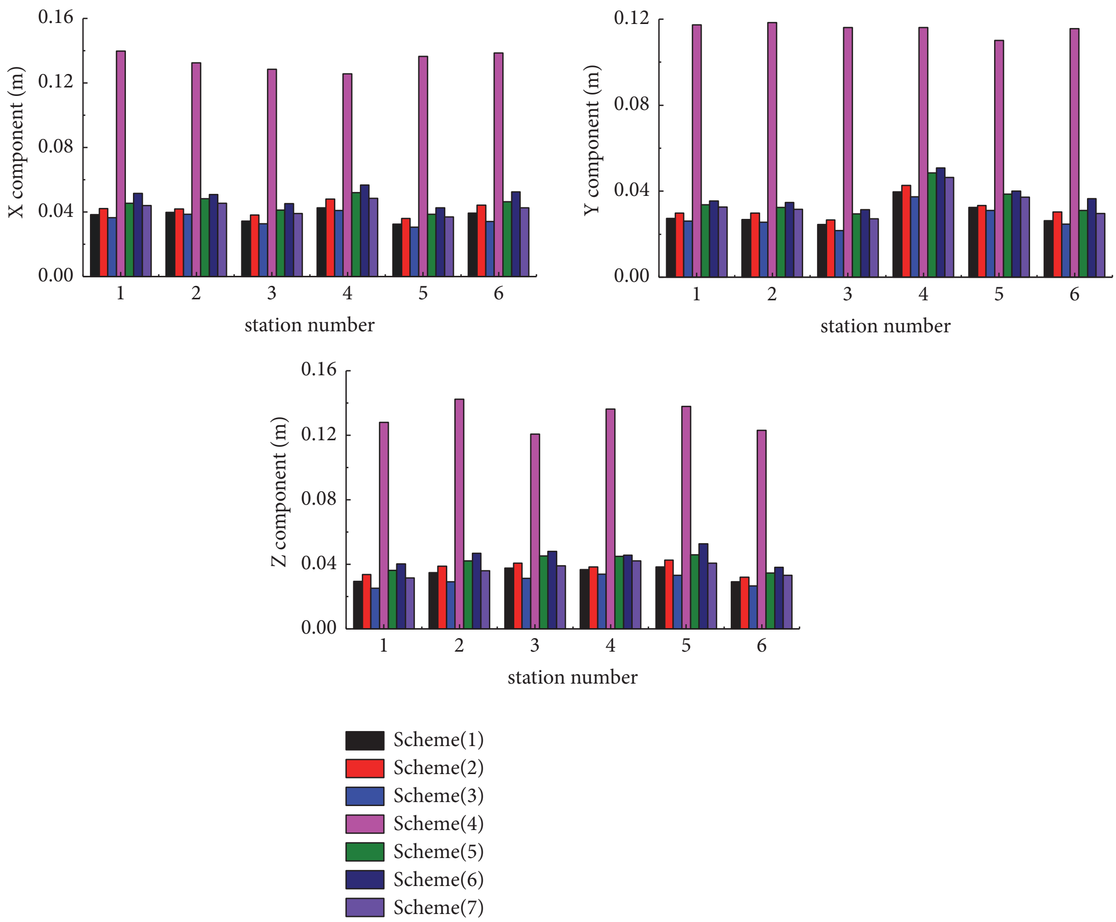

Figure 2: RMSE of the coordinate estimation accuracies in the target frame for the stations in set $\mathbf{\Pi}_2$.

parameters: it not only extends the coverage of the new frame site but also obtains a unified and complete network frame, that is, one that includes coordinate valuation and precision information.

6. Conclusions

In this paper, Helmert transformations among three frames, that is, one target frame and two source frames, were studied as an example. A robust prediction algorithm based on the general EIV prediction algorithm and robust estimation was derived in detail and was applied to achieve multiframe total transformation. Experiments demonstrated that the algorithm proposed in this paper not only effectively avoids the problem of multiple solutions for reference station coordinates by using existing observations to obtain an optimal solution for the total transformation of multiple frames, but also effectively resists interference caused by gross errors. Additionally, we assumed that gross errors can appear in a common station; if a gross error appears in a common station, it can only be eliminated and not solved. Then it will be impossible to solve the coordinates of noncommon stations with gross errors in the target frame; this latter problem will need to be considered in a further in-depth study.

Data Availability

No data were used to support this study.

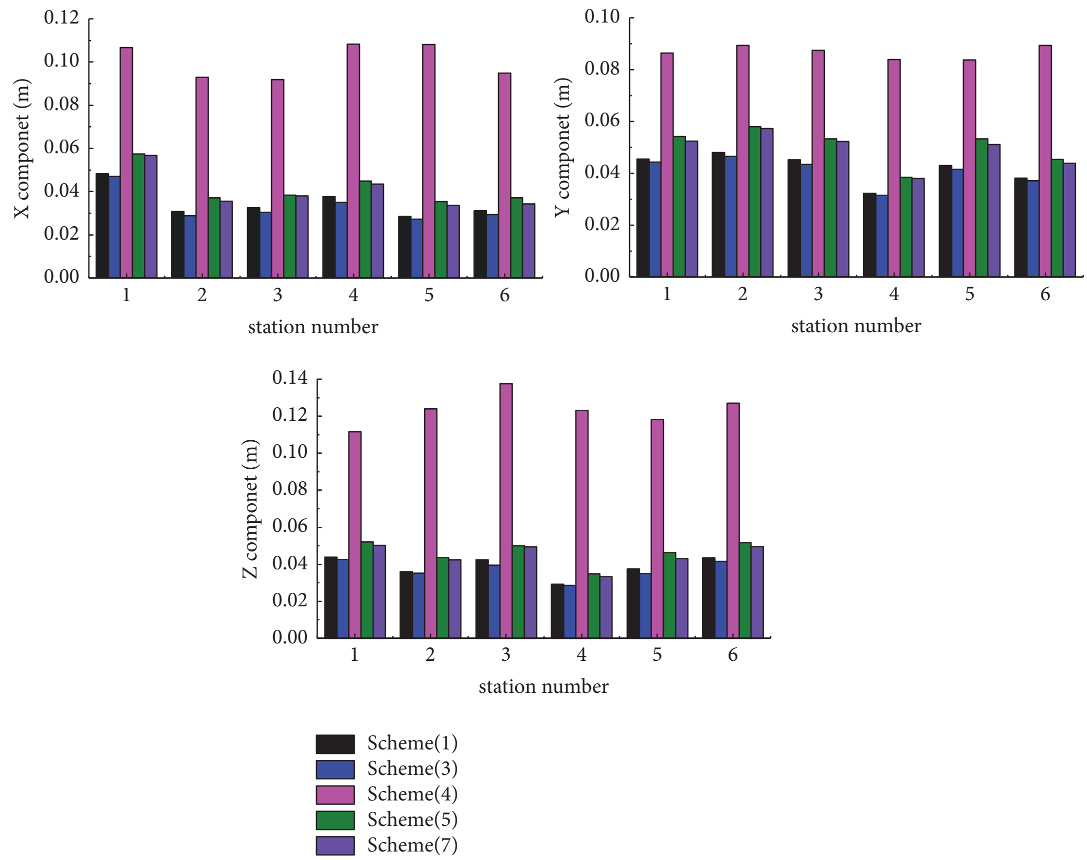

Figure 3: RMSE of the coordinate estimation accuracies in the target frame for the stations in set $\mathbf{\Pi}_3$.

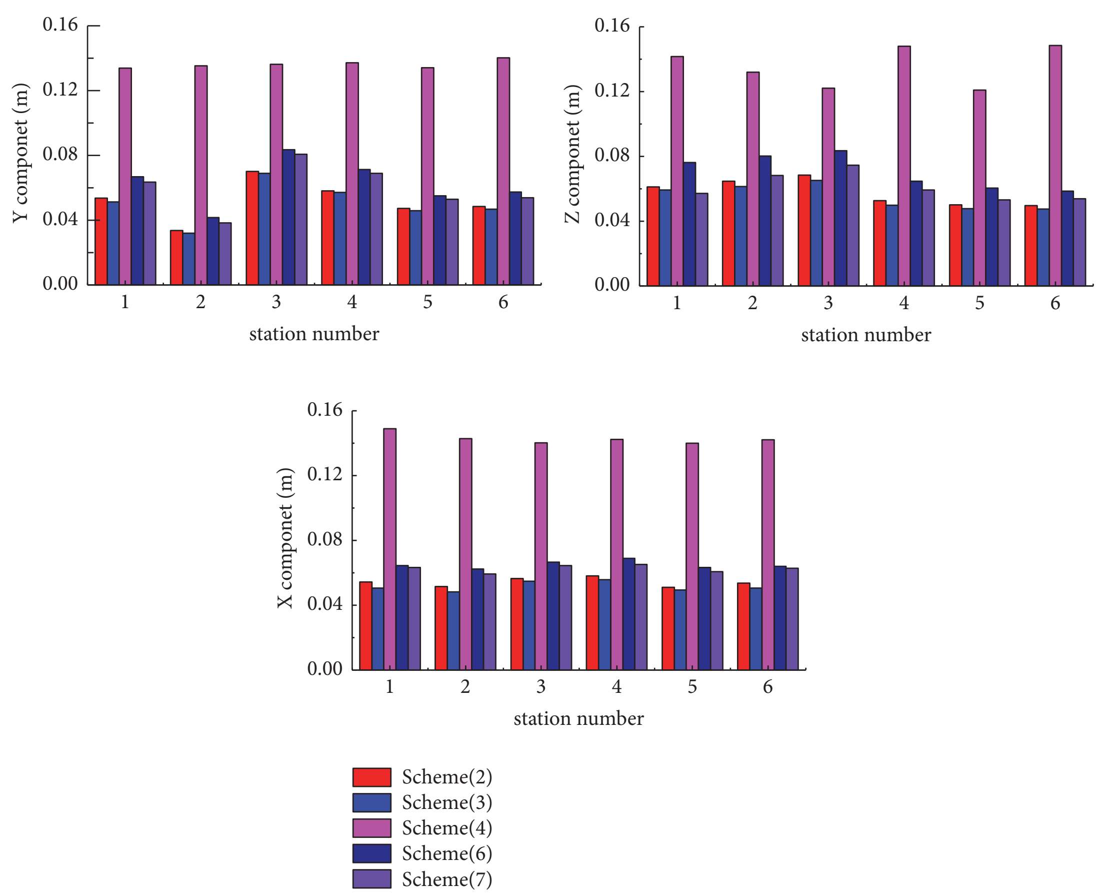

Figure 4: RMSE of the coordinate estimation accuracies in the target frame for the stations in set $\mathbf{\Pi}_4$.

Conflicts of Interest

The authors declare that they have no conflicts of interest.

Authors' Contributions

The authors have made the same contribution. All authors read and approved the final manuscript.

Acknowledgments

This work was jointly supported by the National Natural Science Foundation of China (41604006, 41674006) and the Natural Science Foundation of Jiangsu Province (BK20160247).

References

[1] Q. Zhang, W. Yang, S. Zhang, and L. Yao, "Performance evaluation of QZSS augmenting GPS and BDS single-frequency single-epoch positioning with actual data in Asia-Pacific region," *ISPRS International Journal of Geo-Information*, vol. 7, no. 5, p. 186, 2018.

[2] S. Günter, *Satellite Geodesy: Foundations, Methods and Applications*, Walter de Gruyter, Berlin, Germany, 1993.

[3] X. Fang, "Weighted total least squares: necessary and sufficient conditions, fixed and random parameters," *Journal of Geodesy*, vol. 87, no. 8, pp. 733–749, 2013.

[4] X. Fang, "On non-combinatorial weighted total least squares with inequality constraints," *Journal of Geodesy*, vol. 88, no. 8, pp. 805–816, 2014.

[5] X. Fang, "Weighted total least-squares with constraints: a universal formula for geodetic symmetrical transformations," *Journal of Geodesy*, vol. 89, no. 5, pp. 459–469, 2015.

[6] B. Wang, J. Li, and C. Liu, "A robust weighted total least squares algorithm and its geodetic applications," *Studia Geophysica et Geodaetica*, vol. 60, no. 2, pp. 177–194, 2016.

[7] P. J. G. Teunissen, "The non-linear 2D symmetric helmert transformation: An exact non-linear least-squares solution," *Bulletin Géodésiqué*, vol. 62, no. 1, pp. 1–16, 1988.

[8] M. Acar, M. T. Özlüdemir, O. Akyilmaz, R. N. Çelik, and T. Ayan, "Deformation analysis with total least squares," *Natural Hazards and Earth System Sciences*, vol. 6, no. 4, pp. 663–669, 2006.

[9] A. R. Amiri-Simkooei, C. C. J. M. Tiberius, and P. J. G. Teunissen, "Assessment of noise in GPS coordinate time series: methodology and results," *Journal of Geophysical Research: Solid Earth*, vol. 112, no. 7, pp. 1–19, 2007.

[10] J. Lu, Y. Chen, B. F. Li, and X. Fang, "Robust total least squares with reweighting iteration for three-dimensional similarity transformation," *Survey Review*, vol. 46, no. 334, pp. 28–36, 2014.

[11] Y. A. Felus and R. C. Burtch, "On symmetrical three-dimensional datum conversion," *GPS Solutions*, vol. 13, no. 1, pp. 65–74, 2009.

[12] X. Fang, "A total least squares solution for geodetic datum transformations," *Acta Geodaetica et Geophysica*, vol. 49, no. 2, pp. 189–207, 2014.

[13] G. Chang, "On least-squares solution to 3D similarity transformation problem under Gauss–Helmert model," *Journal of Geodesy*, vol. 89, no. 6, pp. 573–576, 2015.

[14] B. Li and S. Huang, "Analytical close-form solutions for three-dimensional datum transformation with big rotation angles," *Cehui Xuebao/Acta Geodaetica et Cartographica Sinica*, vol. 45, no. 3, pp. 267–273, 2016.

[15] P. Lin, C. Liu, J. Gao, and Y. Yao, "Three-dimensional datum transformation based on Gauss-Helmet model with constraints," *Journal of China University of Mining and Technology*, vol. 46, no. 5, pp. 1152–1158, 2017 (Chinese).

[16] B. Li, "Variance component estimation in the seamless affine transformation model," *Cehui Xuebao/Acta Geodaetica et Cartographica Sinica*, vol. 45, no. 1, pp. 30–35, 2016.

[17] B. Li, Y. Shen, and W. Li, "The seamless model for three-dimensional datum transformation," *Science China Earth Sciences*, vol. 55, no. 12, pp. 2099–2108, 2012.

[18] B. Li, Y. Shen, X. Zhang, C. Li, and L. Lou, "Seamless multivariate affine error-in-variables transformation and its application to map rectification," *International Journal of Geographical Information Science*, vol. 27, no. 8, pp. 1572–1592, 2013.

[19] B. Wang, J. Li, C. Liu, and J. Yu, "Generalized total least squares prediction algorithm for universal 3D similarity transformation," *Advances in Space Research*, vol. 59, no. 3, pp. 815–823, 2017.

[20] P. Lin, G. Chang, J. Gao, Q. Wang, and H. Bian, "Helmert transformation with mixed geodetic and Cartesian coordinates," *Advances in Space Research*, 2017.

[21] J. Y. Han, B. H. W. van Gelder, T. Soler, and R. A. Snay, "Geometric combination of multiple terrestrial network solutions," *Journal of Surveying Engineering*, vol. 134, no. 4, pp. 126–131, 2008.

[22] B. Aktuğ, "Inverse and compound datum/frame transformations," *Journal of Surveying Engineering*, vol. 135, no. 2, pp. 46–55, 2009.

[23] V. Mahboub, A. R. Amiri-Simkooei, and M. A. Sharifi, "Iteratively reweighted total least squares: A robust estimation in errors-in-variables models," *Survey Review*, vol. 45, no. 329, pp. 92–99, 2013.

[24] Z. Lu, Y. Qu, and S. Qiao, *Geodesy: Introduction to Geodetic Datum and Geodetic Systems*, Springer, Berlin, Germany, 2014.

[25] Y.-Q. Tao, J.-X. Gao, and Y.-F. Yao, "TLS algorithm for GPS height fitting based on robust estimation," *Survey Review*, vol. 46, no. 336, pp. 184–188, 2014.

[26] Y. Jin, X. Tong, L. Li, S. Zhang, and S. Liu, "Total least L1- and L2-norm estimations of a coordinate transformation model with a structured parameter matrix," *Studia Geophysica et Geodaetica*, vol. 59, no. 3, pp. 345–365, 2015.

[27] J. Zhao, Q. Gui, and F. Guo, "L1 norm minimization in partial errors-in-variables model," *Acta Geodaetica et Geophysica*, vol. 52, no. 3, pp. 389–406, 2017.

[28] G. Chang, T. Xu, and Q. Wang, "M-estimator for the 3D symmetric helmert coordinate transformation," *Journal of Geodesy*, vol. 92, no. 1, pp. 47–58, 2018.

[29] B. Wang, J. Yu, C. Liu, M. Li, and B. Zhu, "Data snooping algorithm for universal 3D similarity transformation based on generalized EIV model," *Measurement*, vol. 119, pp. 56–62, 2018.

[30] Y. Yang, L. Song, and T. Xu, "Robust parameter estimation for geodetic correlated observations," *Acta Geod Cartograph Sinica*, vol. 31, pp. 95–99, 2002.